CIRP Annals - Manufacturing Technology xxx (2018) xxx–xxx

Contents lists available at ScienceDirect

CIRP Annals - Manufacturing Technology

journal homepage: http://ees.elsevier.com/cirp/default.asp

Semi-analytical modelling with numerical and experimental validation of electromagnetic forming using a uniform pressure actuator

Brad Kinsey *, Shunyi Zhang, Yannis P. Korkolis

Department of Mechanical Engineering, University of New Hampshire, Durham, NH 03824, USA

Submitted by Chris Evans (1), Charlotte, USA

ARTICLE INFO

Keywords:
Forming
Modelling
Electromagnetic deformation

ABSTRACT

In this study, an electromagnetic forming process using a uniform pressure actuator is investigated through electro-magnetic-mechanically coupled numerical simulations; a simplified analytical model to predict the forming pressure and shell theory for mechanical deformation; and experimental results, which include Photon Doppler Velocimetry to measure the deformation. Velocity and the final deformed part shape are compared between the numerical, analytical, and experimental methods and reasonably good agreement is demonstrated. However, accurate comparison is affected by the energy level used with the numerical simulations matching better for the lower energy case due to less material draw-in and the analytical model providing more precise results for the higher energy case.

1. Introduction

Electromagnetic forming (EMF) can be used to plastically deform less ductile materials (e.g., Mg and Al compared to steel), reduce springback [1], and/or create a solid state weld between dissimilar materials [2]. Thus, there are various niche applications in the automotive, aerospace, and biomedical industries for this technology [3]. In EMF, a capacitor bank is charged to a specified energy level, on the order of tens to hundreds of kJ. Then a fast acting switch dissipates the electrical energy, within tens of microseconds, into a specially designed coil. A magnetic field is generated that induces eddy currents in any nearby conductors, including the workpiece. The eddy currents flow in the opposite direction to the applied current creating an opposing magnetic field and accompanying Lorentz force. The workpiece is accelerated away from the coil with a velocity on the order of hundreds of m/s.

Key to the process is the flow of eddy currents in the workpiece to maximize the forming force achieved. Thus, the design of the process and accompanying tooling is critical. For example, Kamal and Daehn [4] created EMF tooling that they designated as a uniform pressure actuator (UPA). See Fig. 1 which includes a die to create microscale features. But this can be replaced by any desired tooling, even an open channel for free forming of the workpiece, as will be presented in this paper. The UPA set-up creates a return path for the eddy currents to flow, thus increasing the strength of the opposing magnetic field and forming force. Without the return path, the eddy currents would simply circulate in the workpiece producing a pressure that would vary spatially and not be as strong near the edges of the workpiece.

EMF is a complicated multiphysics problem with electro-magnetic, mechanical, and thermal components. There are a few commercial software packages that can handle such simulations, e.g., LS-DYNA. Also, simplified analytical models have been developed to predict key process parameters such as magnetic field strength, pressure distribution, velocity of the workpiece, and deformation. For example, analytical models for free tube compression have been studied by multiple researchers with simplifications included to aid calculations. In Weddeling et al. [5], a perfectly plastic material model was used. A more realistic material model was incorporated in Kinsey and Nassiri [6]; however, numerical simulation validation of magnetic pressure was not provided. In both of these studies, good agreement with experimental results was obtained.

Others have considered analytical models for EMF processes of sheets. Hahn et al. [7] welded 5000-series aluminium sheets to a 6000-series aluminium square tubes. In addition to analytically modelling the process, peel tests were conducted to verify the weld strength. Good agreement between the analytical model and experiments was obtained. Thibaudeau and Kinsey [8] created a simplified analytical model for a UPA sheet forming process. While this paper provided an advancement in the state-of-the-art, there were limitations to this work. First, a rigid body assumption was used for the material response. Thus, only a single value for displacement and velocity was predicted, while a distribution is actually observed over the part geometry [8]. This prevented the deformed geometry from being determined, which was also not measured experimentally. Finally, validation of the analytical pressure distribution was not provided.

In this paper, numerical, analytical, and experimental results from a UPA sheet forming process are presented. The numerical simulations provide validation of the electromagnetic predictions of the analytical model, as well as the ability to assess stress and strain values that would otherwise not be determined. The purely analytical model provides a low cost, short cycle time means to

* Corresponding author.
E-mail address: bkinsey@unh.edu (B. Kinsey).

https://doi.org/10.1016/j.cirp.2018.04.028
0007-8506/© 2018 Published by Elsevier Ltd on behalf of CIRP.

investigate a UPA process for a given deformation application. Finally, the experimental results, which included Photon Doppler Velocimetry (PDV) to measure the workpiece velocity and coordinate measurement machine (CMM) data, provide physical values to validate the numerical and analytical approaches. Reasonably good agreement between these three research methods is demonstrated for velocity and displacement.

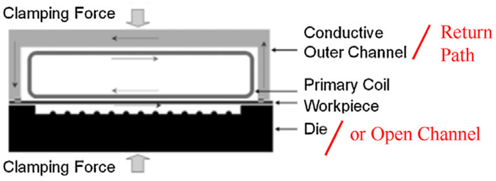

Fig. 1. Uniform pressure actuator concept adapted from Ref. [4].

2. Experimental set-up

Experiments were conducted on a 12 kJ Maxwell Magneform (Model 7000JA) machine. A UPA was fabricated based on analyses to optimize the process [8]. See Fig. 2a for an image of the entire process set-up and Fig. 2b for the coil design. Photon Doppler Velocimetry, which is a laser-based interferometric technique that monitors the shifting or beat frequency of the outgoing and returned laser beam, was used to measure the velocity in the process [9]. The PDV system used in this research has a resolution of 3.2 m/s and is capable of measuring velocities over 500 m/s. The output of the laser detectors was recorded by a LeCroy WaveSurfer WS64MXS-B oscilloscope, with 600 MHz bandwidth, 5GS/s sampling rate, and 16Mpts memory per channel. The PDV probe was targeted at the centre of the workpiece. Retroreflective tape (Nikkalite 48000 series) was attached to the workpiece to assure proper reflection of the laser beam to the detector. The workpiece deformation was measured with a zCAT CMM. The input current to the coil was measured with a Powertek CWT 3000B Rogowski coil, capable of measuring up to 600 kA. See Fig. 3 for the measured currents that were used as input into the numerical simulations. Basic circuit component values, i.e., resistance, inductance, and capacitance, were determined from these current measurements and used in the analytical model as well. To ensure the consistency and repeatability of the experimental measurements, three tests were conducted at two energy levels (3.6 and 6 kJ), with variations shown by the error bars in the experimental results. Fig. 4 shows a deformed workpiece with respect to the coil location along the length direction. Note the oscillating shape with high displacement values at the ends and in the centre of the workpiece. The approximate strain rate during these experiments was 10^3 s^{-1}.

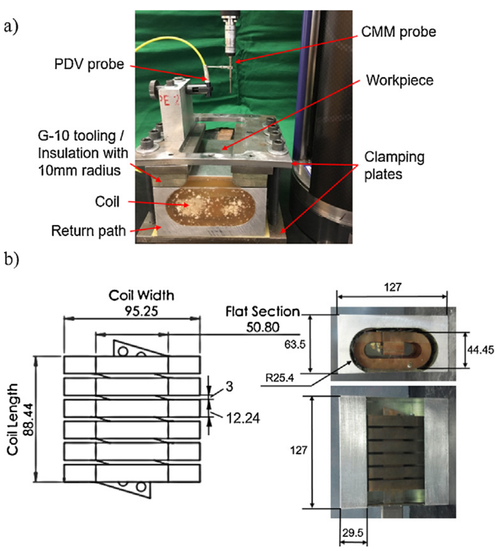

Fig. 2. Experimental (a) set-up and (b) coil geometry.

3. Numerical model

The numerical simulations of the UPA process were conducted in LS-DYNA utilizing the electromagnetism (EM) module [10]. The boundary element method (BEM) in the EM module was used, as this does not require meshing of the surrounding air where the magnetic and electric fields are generated [11]. This method is only applicable for linear partial differential equations, which is an acceptable limitation with small time steps in FEA implementation. In addition to the electromagnetic analyses, the Lorentz force calculated by the EM solver is transferred to a mechanical analysis to deform the conductive workpiece. The change of the gap distance between the coil and the workpiece is taken into account by the Lagrangian computation of the electromagnetic field in the subsequent time increment.

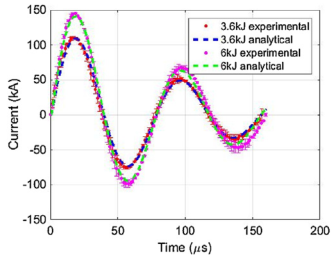

Fig. 3. Experimental and analytically predicted current measurements.

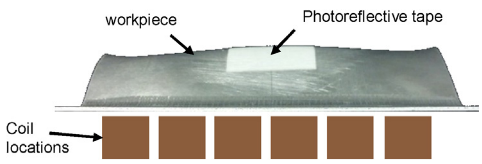

Fig. 4. Deformed workpiece with respect to coil locations.

Fig. 5 shows the numerical model where only the skin depth of the return path was included, as eddy currents only flow in this region. The computational time of the analysis were significantly reduced by this simplification, and the numerical results were not affected. Indicated in Fig. 5 is where measurement data was extracted for comparison of experimental, numerical, and analytical results. There were close to 40,000 elements in the model, with five 3D, reduced integration elements through the thickness of the workpiece. The coil and return path did not deform in the simulations. The experimentally obtained current measurements were used as the input parameter for the EM analysis. The BEM matrix was recalculated every 1 μs and updated to the mechanical solver to capture the influence of sheet deformation on the magnetic field. The workpiece material was AA6061-T6 with the material properties determined from Kolsky Bar tests at various strain rates, 10^0–10^4 s^{-1}, for a power-law hardening material:

$$\overline{\sigma} = C\overline{\varepsilon}^n \dot{\varepsilon}^m \tag{1}$$

where $\overline{\sigma}$, $\overline{\varepsilon}$, and $\dot{\varepsilon}$ are the effective stress, effective strain, and strain rate, respectively, and C, n, and m are material constants. See Table 1.

Fig. 6 shows the pressure distribution obtained from the numerical simulations with respect to time. The six individual coils are clearly visible along the length direction, while the pressure along the width direction is fairly uniform. After the initial large peak values, smaller pressure peaks are observed due to the oscillating current. See Fig. 3.

Table 1
Material properties for AA6061-T6.

C (MPa)	n	m	Density (kg/m^3)	Elastic modulus (GPa)	Poisson's ratio	Electrical resistivity (ohm-nm)
447.2	0.067	0.006	2660	68.9	0.33	39.9